Redox Biology 6 (2015) 326–333

Contents lists available at ScienceDirect

Redox Biology

journal homepage: www.elsevier.com/locate/redox

In vivo parameters influencing 2-Cys Prx oligomerization: The role of enzyme sulfinylation

Y. Noichri [a,1], G. Palais [a,1], V. Ruby [a], B. D'Autreaux [a], A. Delaunay-Moisan [a], T. Nyström [b], M. Molin [b], M.B. Toledano [a,*]

[a] Oxidative Stress and Cancer, IBITECS, SBIGEM, CEA-Saclay, 91191 Gif-sur-Yvette, France
[b] Department of Chemistry and Molecular Biology (CMB), University of Gothenburg, Medicinaregatan 9C, S-413 90 Göteborg, Sweden

ARTICLE INFO

Article history:
Received 25 June 2015
Received in revised form
10 August 2015
Accepted 11 August 2015
Available online 20 August 2015

Keywords:
Peroxiredoxin
H_2O_2
Sulfiredoxin
Peroxidase
Chaperone
S. cerevisiae

ABSTRACT

2-Cys Prxs are H_2O_2-specific antioxidants that become inactivated by enzyme hyperoxidation at elevated H_2O_2 levels. Although hyperoxidation restricts the antioxidant physiological role of these enzymes, it also allows the enzyme to become an efficient chaperone holdase. The critical molecular event allowing the peroxidase to chaperone switch is thought to be the enzyme assembly into high molecular weight (HMW) structures brought about by enzyme hyperoxidation. How hyperoxidation promotes HMW assembly is not well understood and Prx mutants allowing disentangling its peroxidase and chaperone functions are lacking. To begin addressing the link between enzyme hyperoxidation and HMW structures formation, we have evaluated the *in vivo* 2-Cys Prxs quaternary structure changes induced by H_2O_2 by size exclusion chromatography (SEC) on crude lysates, using wild type (Wt) untagged and Myc-tagged *S. cerevisiae* 2-Cys Prx Tsa1 and derivative Tsa1 mutants or genetic conditions known to inactivate peroxidase or chaperone activity or altering the enzyme sensitivity to hyperoxidation. Our data confirm the strict causative link between H_2O_2-induced hyperoxidation and HMW formation/stabilization, also raising the question of whether C_P hyperoxidation triggers the assembly of HMW structures by the stacking of decamers, which is the prevalent view of the literature, or rather, the stabilization of pre-assembled stacked decamers.

1. Introduction

Peroxiredoxins (Prxs) are enzymes that catalyze the reduction of hydrogen peroxide (H_2O_2) *via* a conserved active-site cysteine (Cys) residue. Amongst the six Prx subfamilies, which are distinguished by sequence similarities [32,43], Prx1, also known as typical 2-Cys Prxs, are the most widespread, from archaea, bacteria to eukaryotes. The eukaryotic enzymes of the Prx1 group share with the other family members fast catalytic rates in the order of $\sim 10^7\ M^{-1}\ s^{-1}$ [33,37], but carry the unique property of becoming inactive by hyperoxidation at elevated H_2O_2 levels [45,47,49]. These enzymatic specific attributes determine the unique cellular functions of eukaryotic 2-Cys Prxs as antioxidants, H_2O_2 signaling effectors and controllers, and as chaperones [14].

2-Cys Prx are obligate head-to-tail B-type homodimers, each with two catalytic Cys residues. In the peroxidatic cycle, the N-terminal Cys, named C_P for peroxidatic Cys, reduces H_2O_2, and is in turn oxidized to a sulfenic acid (C_P-SOH) [48] (Fig. 1). The Cys-sulfenic acid moiety then condenses with the C-terminal catalytic Cys residue of the other subunit, or resolving Cys (C_R) into an intermolecular disulfide. In the reduced enzyme C_P and C_R are ~13 Å apart. Therefore, disulfide formation involves an important structural remodeling occurring both at the C_P-active site pocket and C_R-containing C-terminal domain, which switches the enzyme structure form a fully folded (FF) to a locally unfolded (LU) conformation [17,47]. Based on a series of elegant studies Karplus and coworkers have proposed that the enzyme FF conformation both stabilizes the deprotonated reactive form of C_P and provides a steric and electrostatic environment that activates H_2O_2, hence establishing the observed C_P extraordinary high reactivity for H_2O_2[18,22]. The catalytic intermolecular disulfide is subsequently reduced by thioredoxin, which completes the catalytic cycle, and returns the enzyme to the FF conformation. In eukaryotic enzymes however, the C_P-SOH can further react with H_2O_2 instead of condensing with C_R, thus becoming oxidized to the corresponding sulfinic acid ($-SO_2H$), which interrupts the peroxidatic cycle. Hyperoxidized Prx is not a dead-end product; it is reactivated by ATP-dependent reduction of the sulfinate by sulfiredoxin (Srx) [45,6]. The sensitivity of eukaryotic enzymes to hyperoxidation is

* Corresponding author.
E-mail address: Michel.toledano@cea.fr (M.B. Toledano).
[1] These two authors equally contributed to this work.

http://dx.doi.org/10.1016/j.redox.2015.08.011
2213-2317/

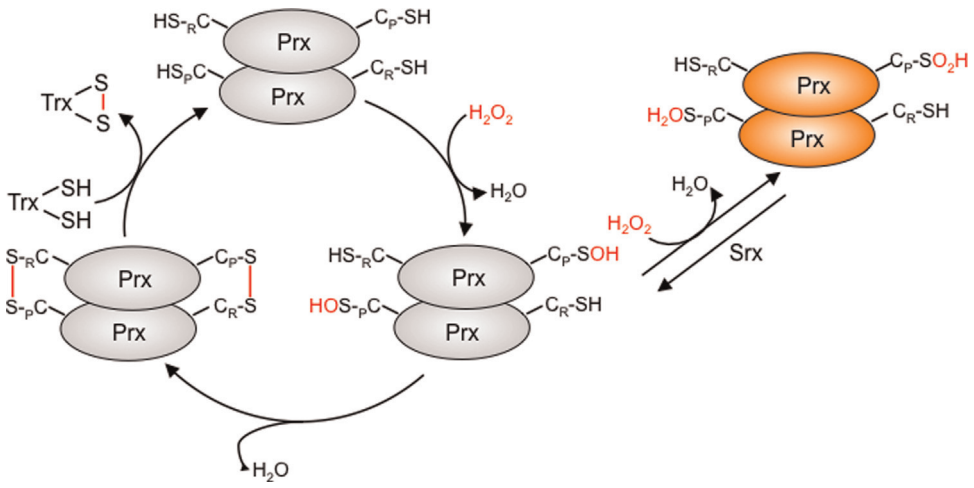

Fig. 1. The peroxidatic cycle of eukaryotic 2-Cys Prxs. Eukaryotic typical 2-Cys Prx are obligate dimers with a mechanism involving two Cys residues, in which C_P decomposes H_2O_2 into H_2O by nucleophilic attack and is oxidized to a sulfenic acid (C_P-SOH). The sulfenic acid then reacts with the resolving Cys (C_R) residue of the other subunit to form an intermolecular disulfide [48]. This disulfide is then reduced by thioredoxin, which completes the catalytic cycle. Alternatively, when H2O2 levels raises, the C_P-SOH can further react with H_2O_2, which leads to formation of a C_P-sulfinic acid (CP-SO_2H). The latter is reversed back to C_P-SOH by ATP-dependent reduction by sulfiredoxin (Srx).

linked to the presence of two sequence fingerprints absent in other family enzymes, a three amino acids insertion in the loop between α4 and β5 associated with a conserved GGLC motif, and an additional helix (α7) occurring as a C-terminal extension and containing the conserved YF motif [47]. Such a structural configuration is thought to slow down the FF to LU transition rate, thereby favoring hyperoxidation [47].

Enzymatic cycling involves dramatic changes in quaternary structure that are crucial for 2-Cys Prxs differential functions. Reduced 2-Cys Prxs is typically in the form of decamers arranged into a ring-like toroid structure constituted of five B-type dimers interacting via their A-type interface [17,41,46,5]. During cycling decamers dissociate into dimers upon disulfide formation and are regained upon disulfide reduction [36,4,46]. As proposed by Karplus and coworkers, there is a reciprocal stabilization between the enzyme in the FF conformation and decamer assembly [17], which explains both that the decamer form enhances catalysis and that catalytic disulfide formation, by locking the enzyme into the LU conformation, dissociates the decamers into dimers [17,46,5,8]. In contrast, enzyme hyperoxidation triggers the stacking of decamers, up to filaments, which stabilize the decameric structure [16,26,38,40,9].

By combining extremely high H_2O_2 reaction rates, reflected by very low K_m values [33], very high expression levels, and the enzyme oxidative inactivation at elevated H_2O_2 levels [45,47,49], 2-Cys Prxs are very efficient towards the low metabolically produced H_2O_2 levels and relatively inefficient towards peroxide onslaughts [14,27]. Concurrently, hyperoxidation constitutes the gateway to the enzyme extra-antioxidant functions, and in particular to its chaperone function.

Jang, Lee and coworkers showed using the two *S. cerevisiae* 2-Cys Prx Tsa1 and Tsa2 *in vitro* that heat or H_2O_2 both promote formation of enzyme high molecular weight (HMW) structures of size > 1000 kDa and of spherical shape that have lost peroxidase activity, but are capable of preventing aggregation of heat-denatured model substrates [20], a function assimilated to that of a chaperone holdase. In the case of H_2O_2, C_P was required for the acquisition of the chaperone function, and sulfiredoxin (Srx1) switched the enzyme back to a low molecular weight (LMW) peroxidase active form by reducing the sulfinate [20,30]. However, C_P was dispensable for heat-induced chaperone activity, which led Jang and coworkers to suggest that heat and H_2O_2 trigger the functional switch of 2-Cys Prx through distinct mechanisms [20]. A chaperone holdase activity similar to Tsa1/2 has now been described for human cytosolic 2-Cys Prxs Prdx1 [19,34,35] and Prdx2 [29], plant chloroplastic 2-Cys Prxs [23], *S. mansoni* 2-Cys Prx SmPrx1 [2,40], *L. infantum* mitochondrial 2-Cys Prx mTXNPx [44], *H.* pylori 2-Cys Prx AhpC [12], cyanobacterial *Anabaena* PCC7120 2-Cys Prx alr4641 [3] and *P. aeruginosa* 2-Cys Prx PaPrx [1]. In most of these cases, the available data fit the model of Jang whereby H_2O_2-induced C_P hyperoxidation promotes formation of 2-Cys Prx HMW structures with chaperone holdase activity, while Srx-dependent sulfinate reduction returns the enzyme to the peroxidatic cycle [20,30]. Note that the Tsa1/2 HMW spherical structures, which have only been described by Jang and colleagues, must somehow be related to the typical decamers stacks, which were shown by others to also carry chaperone activity. The term HMW structures is used thereof to describe multimers > decamers. The above chaperone model does not hold true for the *L. infantum* mitochondrial 2-Cys Prx mTXNPx however [11,44]. In this case, C_P and hence enzyme hyperoxidation is dispensable for chaperone function, and heat but not H_2O_2 triggers within the reduced decamer major conformational changes that increase surface hydrophobicity, without quaternary structure changes. In the case of the *A. thaliana* chloroplastic 2-Cys Prx, although the chaperone function is activated by H_2O_2 and requires C_P sulfinylation, the chaperone active form of the enzyme is a decamer and not a higher order oligomer [23].

In summary, except for the cases of the *L. infantum* mitochondrial and At chloroplastic 2-Cys Prxs, available data support the notion that H_2O_2-induced C_P hyperoxidation activates 2-Cys Prx chaperone function by promoting the stacking of decamers. To elucidate the still unknown physiological scope and mechanism of the chaperone function of 2-Cys Prx *in vivo*, it is important to generate mutations that could unambiguously separate this function from the enzyme peroxidase function, and to establish assays allowing evaluating these mutations. Extensive information on the peroxidatic cycle is now available, which include knowledge of the peroxidatic catalytic site *per se* and the role of and molecular requirements for decamer formation (summarized in [18,22]). In contrast little is know on the link between hyperoxidation and HMW structures formation, which appears as a basic requirement for the chaperone function, and the few available data are very often controversial.

To begin addressing the link between enzyme sulfinylation and HMW structures formation, we have tested whether the *in vivo* quaternary structure of 2-Cys Prxs could be evaluated by size exclusion chromatography on crude lysates. These experiments were performed in *S. cerevisiae* using Tsa1 as model, and mutations known to inactivate chaperone activity or altering the enzyme sensitivity to hyperoxidation. Lysates from cells exposed to H_2O_2 were used to follow the dynamics of enzyme sulfinylation and quaternary structural changes. Data obtained with Tsa1 mutations were compared with those obtained with the same mutations in 2-Cys Prx from other organisms. Our data confirm the strict causative link between H_2O_2-induced sulfinylation and the stabilization of Tsa1 oligomers with a size compatible with that of two-stacked decamers. Our data also suggest that C_P hyperoxidation stabilizes preassembled stacked decamers, rather than triggering the assembly of HMW structures.

2. Results and discussion

2.1. SRX1 overexpression and truncation of YF-containing Tsa1 C-terminal extension abate H_2O_2-induced enzyme sulfinylation

To address the link between 2-Cys Prx sulfinylation and enzyme oligomerization, we selected Tsa1 mutants and genetic conditions predicted to alter enzyme sulfinylation. We used a N-terminal Myc-tagged version of Tsa1 (Myc-Tsa1) [6] and selected three derivative mutants. Myc-Tsa1ΔYF lacks the YF-containing last twelve C-terminal amino acids, and is predicted to be insensitive to sulfinylation, based on data obtained with the *S. pombe* 2-Cys Prx Tpx1 [21,25] human cytosolic Prdx2 [29] and endoplasmic reticulum (ER) Prdx4 [10]; Tsa1^{C48S} carries a serine substitution of C_P, and therefore lacks peroxidase activity, and Tsa1^{C171S} a serine substitution of the resolutive C_R, which has been shown to decrease the sensitivity to sulfinylation of human Prdx4 [10] and *A. thaliana* 2-Cys Prx [23]. Myc-Tsa1 and its corresponding mutants were expressed in a strain lacking Tsa1 (Δ*tsa1*). To appreciate the impact of the N-terminal Myc tag, we also included the analysis of untagged wild type Tsa1 in the corresponding Wt strain. We also included strains lacking *SRX1* (Δ*srx1*) and overexpressing it from the strong CMV promoter in the high-copy episomal plasmid pCM190 (pCM190-SRX1) [15].

We first inspected how Tsa1 mutations and the modulation of *SRX1* expression impacted enzyme sulfinylation by western blots with an anti-Prx$SO_{2/3}$ antibody (Fig. 2). Lysates were prepared before and at different times after cell exposure to 500 μM H_2O_2, a concentration causing full Tsa1 sulfinylation (see Fig. 2G). Sulfinylation of Myc-Tsa1 was maximal at 15 min, started to decrease at 60 min and disappeared at 180 min (Fig. 2A). Myc-Tsa1^{C48S} did not produce any sulfinylation signal, due to the absence of C_P (see Fig. 4B), thus confirming the high specificity of the antibody towards C_P sulfinylation. Myc-Tsa1^{C171S} produced a sulfinylation signal that was 1.5–2 fold lower than Myc-Tsa1 (Fig. 2B), and required twice as much H_2O_2 to reach the levels of sulfinylation seen in Myc-Tsa1 (Fig. 2compare G and H). The lower sensitivity to sulfinylation of Myc-Tsa1^{C171S} is consistent with the effect of the same mutation in *A. thaliana* 2-Cys Prx and human ER Prdx4 [10,23]. Myc-Tsa1ΔYF also produced a sulfinylation signal in response to H_2O_2, but again its intensity was strongly decreased and disappeared much faster than that of Myc-tsa1 (60 *vs* 180 min, compare Fig. 2A and C), thus confirming data obtained with *S. pombe Tpx1*. As the C-Ter domain contributes to the stability of the FF active site conformation, and hence to H_2O_2 reactivity, deleting it affects the sensitivity to sulfinylation by decreasing H_2O_2 reactivity [22]. The same rationale can be made for Myc-Tsa1^{C171S} if we consider that the C_R substitution alters the C-Ter structure. Untagged Wt Tsa1 produced a sulfinylation signal of intensity similar to Myc-Tsa1, but which surprisingly disappeared much faster than that of the tagged enzyme (60 *vs* 180 min, compare Fig. 2A and D). This difference in the enzyme-recycling rate might be explained by an effect of the tag of decreasing Srx enzyme binding or Srx accessibility to the sulfinylated residue. In Δ*srx1,* sulfinylation of untagged Tsa1 at 15 min was indistinguishable form the one seen in Wt cells, but as previously shown [6], the signal remained up to 180 min by lack of enzyme recycling (Fig. 2 compare D and E). In contrast, in cells carrying pCM190-*SRX1*, the sulfinylation signal was barely visible (Fig. 2 compare D and F), which indicate a much faster rate of enzyme recycling by virtue of Srx1 overexpression.

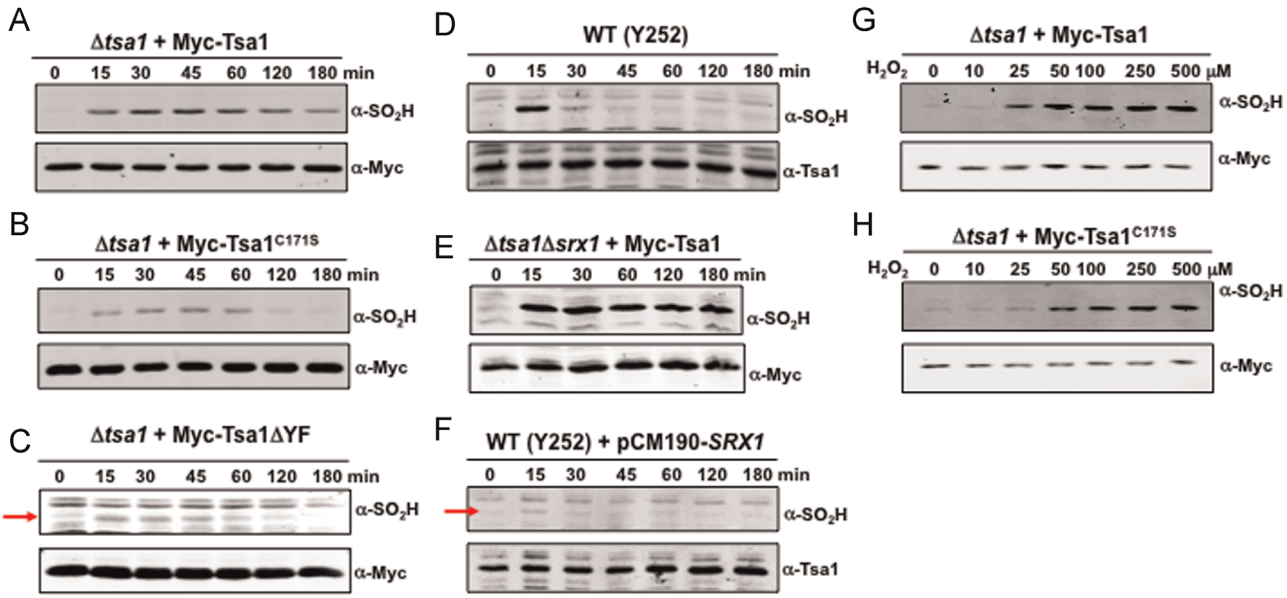

Fig. 2. Evaluation of the sensitivity to sulfinylation of Tsa1 and derivative mutants. TCA-precipitated lysates from, Δ*tsa1* (A–C, G and H) or in Δ*tsa1*Δ*srx1* (E) or in Wt (D and F) yeast cells expressing Myc-Tsa1, MycTsa1^{C48S}, Myc-Tsa1^{C171S}, Myc-Tsa1ΔYF or overexpressing *SRX1*, as indicated, which were exposed to H_2O_2 (500 μM) (A–F), or to the indicated amount of H_2O_2 during 15 min (G and H) were resolved by reducing SDS PAGE, followed by western blot using the anti-Myc, anti-Tsa1 or anti-$SO_{2/3}$ antibodies, as indicated. The red arrow indicates the sulfinylation signal band.

2.2. H_2O_2 triggers the reversible oligomerization of Myc-Tsa1 into the size of two decamers

To analyze the *in vivo* oligomeric state of Myc-Tsa1, we performed size exclusion chromatography on N-ethylmaleimide (NEM)-treated crude cell extracts from Myc-Tsa1-expressing Δ*tsa1* cells that were left untreated or were exposed to H_2O_2 (500 μM) for 15 and 180 min. Collected fractions were resolved by SDS-PAGE in which reducing agents were omitted in order to simultaneously evaluate disulfide-linked homodimer formation. Western blots were probed with anti-Myc and anti-$PrxSO_{2/3}$ antibodies (Fig. 3A). In untreated cells lysates, Myc-Tsa1 largely eluted at a size between that of a monomer (theoretical molecular weight of 21.5 kDa) and dimer (43 kDa), with traces of it equally distributed in all fractions, up to the column size exclusion (670 kDa). Myc-Tsa1 was mostly in the disulfide-linked dimer form, but these disulfides had probably formed after lysis, due to incomplete free sulfhydryls quenching, since Myc-Tsa1 from trichloroacetic acid (TCA)-precipitated lysates from the same cells largely migrated as a reduced monomer (not shown). As expected, probing membranes with the anti-$PrxSO_{2/3}$ did not yield any signal. In lysates from the 15 min H_2O_2 exposure sample, half of Myc-Tsa1 now eluted at about the 27 kDa elution control, close to the size of monomeric enzyme (21.5 kDa), and the other half at a size of about 500 kDa, which is compatible with that of two-stacked Myc-Tsa1 decamers, also referred from now on to the high molecular weight (HMW) form. A chromatogram of standard molecular weight markers is shown in Fig. 3C. Disulfide-linked dimers were here almost totally absent, as a consequence of enzyme sulfinylation, as also shown by probing membranes with the anti-$PrxSO_{2/3}$ antibody that revealed intense signals. Sulfinylation was equally distributed in fractions corresponding to the monomeric and HMW forms. Remarquably, in lysates from the 180 min H_2O_2 exposure sample, the Myc-Tsa1 elution pattern resembled now to that of untreated cells. Still, a strong sulfinylation signal persisted in Myc-Tsa1 monomers. We similarly analyzed the elution of Myc-Tsa1 from Δ*srx1* lysates (Fig. 3B). Elution of Myc-Tsa1 from lysates of untreated cells resembled the one observed in WT untreated cells, except for a smaller proportion of monomeric enzyme and the presence of a small proportion of the enzyme in the HMW form. In lysates of the 15 min H_2O_2 exposure sample, elution of Myc-Tsa1 had also a wild type pattern, except for a higher abundance of the HMW species. In lysates of the 180 min sample however, the major fraction of Myc-Tsa1 now remained in the sulfinylated HMW form, in contrast to what was observed in WT cells.

In summary, in untreated cells Myc-Tsa1 mainly exists as a non-covalently-linked dimer, with H_2O_2 triggering its reversible oligomerization into a HMW form of size compatible with two-stacked decamers, while undergoing reversible sulfinylation. In Δ*srx1*, H_2O_2 also triggers the oligomerization of Myc-Tsa1 to the two-stacked decamers form, but the enzyme remains in this form presumably by lack of sulfinate reduction. Myc-Tsa1 oligomeric transitions are consistent with those observed with untagged Tsa1 by native PAGE, also showing formations of HMW forms in response to H_2O_2 and their reversion upon Srx1 sulfinate reduction [30].

2.3. Ser substitution of peroxidatic Cys stabilizes the Myc-Tsa1 two-stacked decamer

We next analyzed Myc-Tsa1 catalytic Cys mutants, also expressed in Δ*tsa1*. Myc-Tsa1^{C171S} had an elution profile resembling

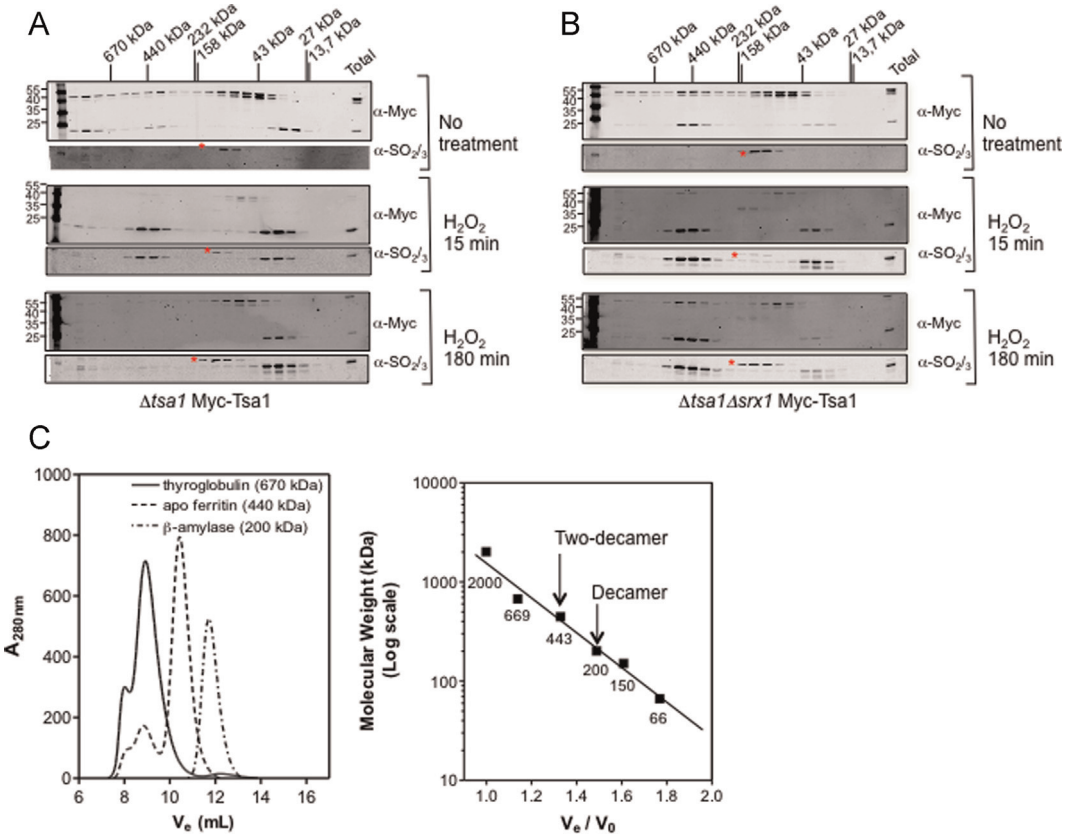

Fig. 3. SEC elution profile of Myc-Tsa1 and the effect of inactivating *SRX1* on the enzyme quaternary structure. Crude lysates from Δ*tsa1* (A) or in Δ*tsa1*Δ*srx1* (B) cells expressing Myc-Tsa1 were taken before and after exposure to H_2O_2 (500 μM) for the indicated time and resolved by SEC. Elution fractions were resolved by non-reducing SDS PAGE, followed by western blot using the anti-Myc or anti-$SO_{2/3}$ antibody as indicated. The elution fraction of standard molecular weight markers is represented at the top of the gel. The red star indicates non-specific signals revealed by the anti-$SO_{2/3}$ antibody. (C) Representative chromatogram of standard molecular weight markers, thyroglobulin (670 kDa), apoferitin (443 kDa), β-amylase (200 kDa) to help resolve the size of the two-stacked decamers.

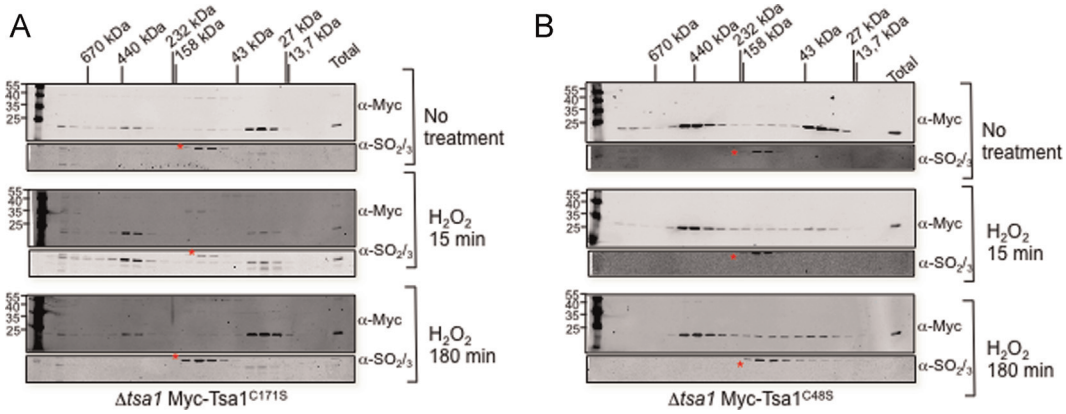

Fig. 4. SEC elution profile of Myc-Tsa1^{C171S}and Myc-Tsa1^{C48S}. Crude lysates from Δ*tsa1* cells expressing Myc-Tsa1C^{171S} (A) or Myc-Tsa1^{C48S} (B) were taken before and after exposure to H_2O_2 (500 μM) for the indicated time and resolved by SEC. Elution fractions were resolved by non-reducing SDS PAGE, followed by western blot using the anti-Myc or anti-$SO_{2/3}$ antibody as indicated. The elution fraction of standard molecular weight markers is represented at the top of the gel. The red star indicates non-specific signals revealed by the anti-$SO_{2/3}$ antibody.

that of Wt enzyme, except for its weaker sulfinylation, in keeping with the data of Fig. 2, and for the reversion of the HMW form at 180 min after H_2O_2 exposure that was not as complete. As predicted, this mutant did not form any disulfide-linked dimer by lack of C_R. Myc-Tsa1^{C48S} in contrast had a strikingly different behavior. Elution of this mutant from untreated cell lysates resembled the elution of Myc-Tsa1 from the 15 min H_2O_2 exposure sample, with half of the protein in the monomeric form and the other half in the HMW form. Further, 15 min after H_2O_2 exposure, most of Myc-Tsa1^{C48S} was now shifted to the HMW form, thus indicating that despite lack of C_P the enzyme retained the ability to respond to H_2O_2. Lastly at 180 min, the protein still eluted for its major part at the HMW size, indicating lack of reversibility. As noticed above, this mutant did not give any sulfinylation signal, and as Myc-Tsa1^{C171S} did not form the disulfide-linked dimer.

In summary, Myc-Tsa1^{C171S} is less prone to sulfinylation, presumably by decreased H_2O_2 reactivity (see above). Further, it fully assembles into the HMW form that might be more stable than that of the Wt tagged enzyme. This latter result should be considered in view of the observation by native PAGE that the same Tsa1 mutant, but without any tag, is constitutively present in the HMW form prior to exposure to H_2O_2 [20], and of the same mutant in *A. thaliana* 2-Cys Prx the decameric form of which is more stable [23,24]. Myc-Tsa1^{C48S} is already in the HMW form prior to exposure to H_2O_2, in keeping with the behavior of the same mutation in purified *S. mansoni* 2-Cys Prx SmPrx1 [2] and purified bovine mitochondrial 2-Cys Prx SP-22 [16], which both eluted during SEC as HMW species, and were seen as long filaments of multiple decamer stacks by transmission electron microscopy. However our data disagree with native PAGE analysis data of the same Tsa1 and of human Prdx2 mutants showing they could not assemble into a HMW form in response to H_2O_2 [20,29]. The basis of these discrepant results is not clear. The stability of 2-Cys Prx with a Ser substitution of C_P raises the question of the structural determinants allowing formation of HMW structures that remains still poorly understood and controversial [2,39]. Another peculiar phenotype of Myc-Tsa1^{C48S} observed here is its ability to further switch its quaternary structure to the HMW form in response to H_2O_2, which might indicate either another 2-Cys Prx H_2O_2-responsive domain in addition to C_P or the presence of an unknown H_2O_2 responsive factor helping Tsa1 HMW assembly.

2.4. The N-Ter tag destabilizes Tsa1 HMW structures

The presence of an N-terminal tag has previously been shown to modify the function of 2-Cys Prxs [8]. That the Myc tag also alters the function of Tsa1 was already suggested by the inability of Myc-Tsa1 to fully rescue the H_2O_2 tolerance of a Δ*tsa1* strain (unpublished data), and by the slower recycling of the sulfinylated enzyme (see Fig. 1). We thus assayed the elution profile of untagged Tsa1 (Fig. 5). Untagged Tsa1 elution pattern was quite different from that of the Myc-tagged enzyme, since more than half of it was in the HMW form (70%), and the remainder in the monomer-dimer form. At 15 min after H_2O_2 exposure, the HMW form switched to the monomer-dimer form, which resulted in equal amounts of enzymes in these two forms; at 180 min, the elution pattern had returned to that of untreated cells, but with a slightly higher amount of protein, as a probable result of gene induction. Traces of the sulfinylation signal were seen at 15 min.

Comparison of Tsa1 and Myc-Tsa1 elution profiles strongly suggests that the N-Terminal Myc tag destabilizes the HMW forms of the enzyme, despite a protracted sulfinylation in Myc-Tsa1. These data are fully consistent with those of bovine mitochondrial Prdx3 (or known as SP-22), in which removal of the N-terminal His

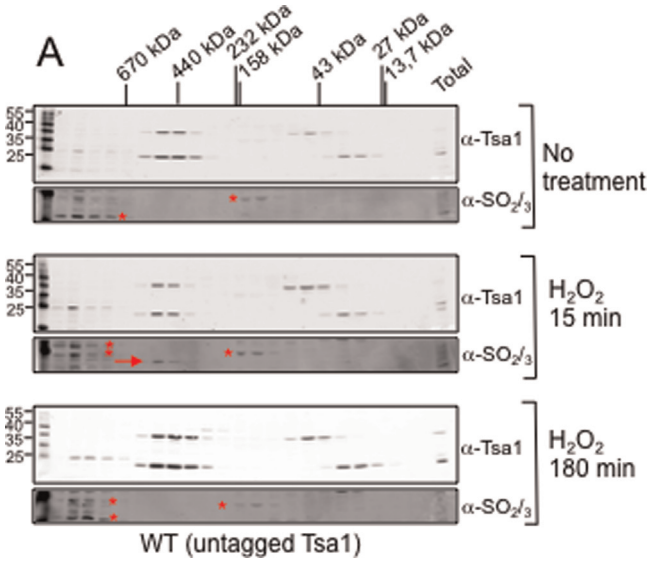

Fig. 5. SEC elution profile of untagged Tsa1. Crude lysates from Wt cells were taken before and after exposure to H_2O_2 (500 μM) for the indicated time and resolved by SEC. Elution fractions were resolved by non-reducing SDS PAGE, followed by western blot using the anti-Myc or anti-$SO_{2/3}$ antibody as indicated. The elution fraction of standard molecular weight markers is represented at the top of the gel. The red star indicates non-specific signals revealed by the anti-$SO_{2/3}$ antibody.

tag stimulated the enzyme peroxidase activity by 3–4 fold, but also destabilized the dodecameric form of the enzyme [8], and with those of the *A. thaliana* chloroplastic 2-Cys Prx in which the N-terminal His tag also decreased peroxidase activity, but also increased the enzyme sensitivity to hyperoxidation [23]. In contrast, the *in vitro* dimer to decamer equilibrium of the *L. braziliensis* mitochondrial 2-Cys Prx *Lb*Prx1m (similar to *L. infantum* mitochondrial 2-Cys Prx mTXNPx) is not altered by the N-terminal His tag [31]. However in the latter case, lowering the pH to acidic conditions was used to alter enzyme quaternary structure instead of protein redox changes as in our assay, which make the comparison irrelevant.

2.5. Myc-Tsa1ΔYF and SRX1 promote entry into the peroxidatic cycle

We next evaluated Myc-Tsa1ΔYF and the effect of overexpressing *SRX1* on the untagged enzyme, both conditions abating enzyme sulfinylation. Myc-Tsa1ΔYF had a unique elution pattern (Fig. 6A). Prior to H_2O_2 exposure, a large proportion of the protein eluted at the size of the two-stacked decamers, and about a quarter of it in the disulfide-linked dimer form. Then, 15 min after H_2O_2 exposure, Myc-Tsa1ΔYF was almost totally shifted to the monomer-dimer size, with about more than half of the protein in the disulfide-linked dimer form. At 180 min, the protein had entirely returned to the double decamer form. Elution of untagged Tsa1 from lysates of cells overexpressing *SRX1* was very similar to that of Myc-Tsa1ΔYF since prior to H_2O_2 exposure, a major part of it also eluted in the HMW form, but then was almost completely switched to the monomer-dimer form after 15 min of H_2O_2 exposure to completely return to the HMW form after 180 min (Fig. 6B). Note that in lysates of *SRX1*-overexpressing cells exposed for 15 min to H_2O_2 untagged Tsa1 eluted exclusively as a disulfide-linked dimer, whereas in Wt cells it was about equally distributed between a disulfide-linked dimer and a monomer. As expected from the results of Fig. 2, for both Myc-Tsa1ΔYF and *SRX1* overexpression no sulfinylation signal was seen.

In summary, both the deletion of the C-terminal-containing YF motif and the over expression of *SRX1* increase the enzyme proportion in the HMW under steady state, prior to exposure to H_2O_2 (compare Fig. 6 and the Myc-Tsa1 elution profile in Fig. 3A), while completely switching it to the dimer-monomer form in response to H_2O_2. These two genetic conditions both increase the enzyme overall peroxidase efficiency by preventing its inactivation, and therefore must result in lowered cellular H_2O_2 levels at steady state, compared to Myc-Tsa1 expressing cells. Decreased steady state cellular H_2O_2 levels might decrease the rate at which the enzyme is brought into the peroxidatic cycle, i.e. in the dimer-monomer form, hence keeping it in the HMW form. In contrast, in response to H_2O_2 the enzyme remains in the peroxidatic cycle, iteratively disassembling the HMW forms upon disulfide bond formation, hence keeping it in the dimer-monomer form. Of note, deleting the YF-containing C-terminal 2-Cys Prx domain, while it significantly decrease sensitivity to hyperoxidation, does not prevent formation of the two-stacked decamer form, which fit those of a similar mutation in *S. mansoni* 2-Cys Prx SmPrx1 that assembled as a stable double decamer [2], but not with those of *A. thaliana* 2-Cys Prx and human Prdx2, the C-Ter deletion of which were shown unable to assemble as a decamer or as HMW structure in response to H_2O_2, respectively [23,29]. Based on the crystal structure of a double decamer, Angelucci and coworkers have suggested that the C-Ter domain sterically prevents the stacking of two decamers when folded, and must therefore be disordered for stacking, which would explain why its removal favors HMW assembly [2,40]. However, a recent cryo-microscopic study of filaments of human Prdx3 obtained at acidic pH indicates that the C-ter domain appears well structured [39].

3. Conclusion

The 2-Cys Prxs family enzymes are H_2O_2-specific antioxidants that carry the unusual feature of enzyme oxidative inactivation at elevated H_2O_2 levels. Although it restricts H_2O_2 scavenging efficiency, inactivation of the enzyme by hyperoxidation constitutes the gateway to its extra-antioxidant functions, and in particular its ability to operate as very efficient chaperone holdases [20]. The critical molecular event allowing the switch from a peroxidase to a chaperone is believed to be the enzyme assembly into HMW structures formed by the stacking of decamers up to filaments, an event that correlates with enzyme hyperoxidation. However, although enzyme hyperoxidation promotes HMW assembly and/or stabilizes these structures, how this event occurs at the molecular level is yet unknown.

To begin answering this question, we have here evaluated the relationship between enzyme quaternary structure and its hyperoxidation *in vivo* by SEC. A salient result of this set of

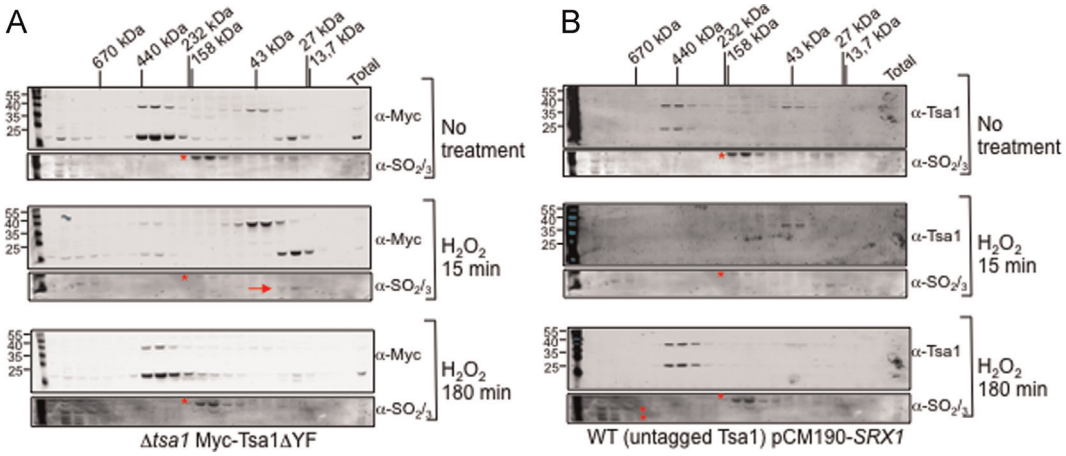

Fig. 6. SEC elution profile of Myc-Tsa1ΔYF and the effect of overexpressing *SRX1*on Tsa1 quaternary structure. Crude lysates from Δ*tsa1* cells expressing Myc-Tsa1ΔYF (A) or Wt overexpressing *SRX1* (B) were taken before and after exposure to H_2O_2 (500 μM) for the indicated time and resolved by SEC. Elution fractions were resolved by non-reducing SDS PAGE, followed by western blot using the anti-Myc or anti-$SO_{2/3}$ antibody as indicated. The elution fraction of standard molecular weight markers is represented at the top of the gel. The red star indicates non-specific signals revealed by the anti-$SO_{2/3}$ antibody.

experiments is the observation that depending on the conditions, Tsa1 elutes as two distinct oligomeric forms, as a disulfide-linked or non-covalently linked dimer, assuming the latter form dissociates during SDS-PAGE, and as a HMW forms that we interpret is constituted of two-stacked decamers. As inferred by combining the data obtained with the native untagged enzyme the Myc-Tagged one, the latter having the advantage of exacerbating quaternary structures changes by decreasing the stability of the HMW form, we propose that Tsa1 exist in cells as a relatively instable two-stacked decamer (seen with native Tsa1 but not with Myc-Tsa1). Exposure to H_2O_2 leads to two outcomes: (i) with untagged and tagged Wt enzymes, after a few peroxidatic cycles C_P becomes hyperoxidized, which stabilizes the HMW form, now also seen with Myc-Tsa1, until the enzyme is recycled by Srx1 that returns it to the relatively instable HMW form; (ii) under conditions preventing sulfinylation, i.e. Myc-Tsa1ΔYF and *SRX1* overexpression, the enzyme is instead kept in the dimer-monomer form by entering into iterative peroxidatic cycles, which breaks apart the HMW form until resolution of the H_2O_2 onslaught. Jang, and coworkers used native PAGE to monitor the changes in enzyme quaternary structure triggered by H_2O_2, and showed the presence of two main oligomeric forms of undefined size, one of which must be the dimeric enzyme and the other presumably the two-stacked decamers [20,30]. We confirm here these data, and also provide a visualization of the alternative enzyme paths. We also further demonstrate the causative link between HMW formation/stabilization and C_P sulfinylation. Furthermore, provided that our estimate of the size of the observed HMW as a two-stacked decamer is correct, our data raise the question of whether C_P hyperoxidation triggers the assembly of HMW structures by the stacking of decamers, a view that reflects the literature, or as suggested here, the stabilization of preassembled stacked decamers. Our study also provides the effects of specific mutations on Tsa1 sensitivity to hyperoxidation and on its quaternary structural changes. These mutants and the SEC assay on crude lysates used here should help contribute to disentangle the intricate function of 2-Cys Prxs as antioxidants and chaperone holdases.

4. Experimental procedures

4.1. Yeast strains, plasmids, growth media and standard methods

The *S. cerevisiae* strains used here are Y252 (Mat**a***ura3-52 lys2-801^{amber}ade2-101^{ochre}trp1-Δ1 leu2-Δ1*) [42], and BY4741 [7] and derivatives (listed in Table 1). Cells were grown at 30 °C in YPD (1% yeast extract, 2% peptone and 2% glucose), or minimal media (SD) (0.67% yeast nitrogen base w/o amino acids, 2% glucose), with amino acid supplements as appropriate. The plasmids used in this study are pRS316-Myc-Tsa1 [6] and derivative pRS316-Myc-TSA1^{C48S} and pRS316-Myc-TSA1^{C171S}, that were generated by standard PCR-mediated site-directed mutagenesis using pRS316-Myc-TSA1 as template [28]; pRS316-Myc-Tsa1YF was similarly prepared by deleting the sequence encoding c-terminal last 11 amino acids before codon stop; for pCM190-SRX1, the PCR-amplified *SRX1* ORF was cloned between PmeI and NotI downstream of the *CYC1*-tetracycline-regulatable promoter of pCM190 [15].

Table 1
Genotype of the *S. cerevisiae* strains used in this study

Strain	Genotype	Reference source
Y252	Mat**a** *ura3-52 lys2-801^{amber}ade2-101^{ochre}trp1-Δ1 leu2-Δ1*	
BY4741	Mat**a** *his3Δ0 leu2Δ0 met15Δ0 ura3Δ0*	
BY4742	Mat**a** *his3Δ0 leu2Δ0 lys2Δ0 ura3Δ0*	
Δ*tsa1*	BY4741 *tsa1D::kanMX4*	This work
Δ*srx1*	*srx1Δ::kanMX4*	This work
D*tsa1*D*srx1*	BY4741 *srx1D::natMX4 tsa1D::kanMX4*	This work

4.2. Size exclusion chromatography

For extracts preparation, the pellets of exponentially growing cell cultures were resuspended in lysis buffer [PBS pH 7.8, NEM 50 mM, PMSF, Complete protease inhibitors cocktail (ROCHE)] at a density of 2.4×10^6 cellules/mL. Cells were lysed on a Constant Cell Disruption Systems (CCDS, One Shot, CellD) under a pressure of 2500 bar. Lysates were centrifuged at 10,000*g*, 4 °C for 10 min, and the supernatant (100 mL) applied on a Superdex 200 10/300 GL (GE Healthcare) column pre-calibrated using a solution of thyroglobulin (670 kDa), apoferritin (443 kDa), catalase (232 kDa), β-amylase (200 kDa), aldolase (158 kDa), ovalbuline (43 kDa), chymotrypsinogene A (27 kDa) and ribonuclease A (13 kDa). Chromatography was performed by High Performance Liquid Chromatography on an AKTA purifier (AmershamPharmaciaBiotec) at a rate of 500 μL/min at room temperature. PBS was used for the elution.

4.3. Western blot

For analysis of enzyme sulfinylation, lysates were prepared by the TCA lysis protocol, and separated by reducing 12 % SDS-PAGE, as described [13]. For analysis of SEC eluates, collected fractions (500 μL) were concentrated on a StrataClean resin (10 mL), proteins were eluted from the resin into Laemli buffer [2% SDS, 62.5 mM Tris–HCl pH 8.7, 10% glycerol, 0.01% bromophenol blue], assessed for protein content, and loaded on non-reducing 12% SDS-PAGE. Gels were then transferred to a nitrocellulose membrane. Membranes were probed with the following primary antibodies anti-Myc (9E10), anti-Tpx1 (a gift from Drs Yang Sol Lee and Ho Hee Jang, Korea), and anti-Prx-$SO_{2/3}$ (Ab16830, Abcam), which were revealed using fluorescent anti-mouse IgG or anti-rabbit IgG secondary antibodies and analyzed on the Odyssey infrared imaging system and software (Odyssey, LI-COR).

Acknowledgement

We are indebted to Dr. Sue Goo Rhee, Sang Yeol Lee, Ho Hee Jang and Ho Zoon Chae for the gifts of anti-Tsa1 and anti-$SO_{2/3}$ antibodies. This work was funded by grant from ANR ERRed and InCA PLBIO INCA_5869 to MBT, and supported by COST Action BM1203 (EU-ROS).

References

[1] B.C. An, S.S. Lee, E.M. Lee, J.T. Lee, S.G. Wi, H.S. Jung, W. Park, B.Y. Chung, A new antioxidant with dual functions as a peroxidase and chaperone in *Pseudomonas aeruginosa*, Mol. Cells 29 (2010) 145–151.
[2] F. Angelucci, F. Saccoccia, M. Ardini, G. Boumis, M. Brunori, L. Di Leandro, R. Ippoliti, A.E. Miele, G. Natoli, S. Scotti, et al., Switching between the alternative structures and functions of a 2-Cys peroxiredoxin, by site-directed mutagenesis, J. Mol. Biol. 425 (2013) 4556–4568.
[3] M. Banerjee, D. Chakravarty, A. Ballal, Redox-dependent chaperone/peroxidase function of 2-Cys-Prx from the cyanobacterium Anabaena PCC7120: role in oxidative stress tolerance, BMC Plant Biol. 15 (2015) 60.
[4] S. Barranco-Medina, S. Kakorin, J.J. Lazaro, K.J. Dietz, Thermodynamics of the dimer-decamer transition of reduced human and plant 2-cys peroxiredoxin, Biochemistry 47 (2008) 7196–7204.
[5] S. Barranco-Medina, J.J. Lazaro, K.J. Dietz, The oligomeric conformation of peroxiredoxins links redox state to function, FEBS Lett. 583 (2009) 1809–1816.
[6] B. Biteau, J. Labarre, M.B. Toledano, ATP-dependent reduction of cysteine-sulphinic acid by *S. cerevisiae* sulphiredoxin, Nature *425* (2003) 980–984.
[7] C.B. Brachmann, A. Davies, G.J. Cost, E. Caputo, J. Li, P. Hieter, J.D. Boeke, Designer deletion strains derived from *Saccharomyces cerevisiae* S288C: a useful set of strains and plasmids for PCR-mediated gene disruption and other

applications, Yeast 14 (1998) 115–132.
[8] Z. Cao, D. Bhella, J.G. Lindsay, Reconstitution of the mitochondrial PrxIII antioxidant defence pathway: general properties and factors affecting PrxIII activity and oligomeric state, J. Mol. Biol. 372 (2007) 1022–1033.
[9] Z. Cao, A.W. Roszak, L.J. Gourlay, J.G. Lindsay, N.W. Isaacs, Bovine mitochondrial peroxiredoxin III forms a two-ring catenane, Structure *13* (2005) 1661–1664.
[10] Z. Cao, T.J. Tavender, A.W. Roszak, R.J. Cogdell, N.J. Bulleid, Crystal structure of reduced and of oxidized peroxiredoxin IV enzyme reveals a stable oxidized decamer and a non-disulfide-bonded intermediate in the catalytic cycle, J. Biol. Chem. 286 (2011) 42257–42266.
[11] H. Castro, F. Teixeira, S. Romao, M. Santos, T. Cruz, M. Florido, R. Appelberg, P. Oliveira, F. Ferreira-da-Silva, A.M. Tomas, Leishmania mitochondrial peroxiredoxin plays a crucial peroxidase-unrelated role during infection: insight into its novel chaperone activity, PLoS Pathog. 7 (2011) e1002325.
[12] M.H. Chuang, M.S. Wu, W.L. Lo, J.T. Lin, C.H. Wong, S.H. Chiou, The antioxidant protein alkylhydroperoxide reductase of *Helicobacter pylori* switches from a peroxide reductase to a molecular chaperone function, Proc. Natl. Acad. Sci. USA 103 (2006) 2552–2557.
[13] A. Delaunay, A.D. Isnard, M.B. Toledano, H_2O_2 sensing through oxidation of the Yap1 transcription factor, EMBO J. 19 (2000) 5157–5166.
[14] S. Fourquet, M.E. Huang, B. D'Autreaux, M.B. Toledano, The dual functions of thiol-based peroxidases in H_2O_2 scavenging and signaling, Antioxid. Redox Signal. 10 (2008) 1565–1576.
[15] E. Gari, L. Piedrafita, M. Aldea, E. Herrero, A set of vectors with a tetracycline-regulatable promoter system for modulated gene expression in *Saccharomyces cerevisiae*, Yeast 13 (1997) 837–848.
[16] L.J. Gourlay, D. Bhella, S.M. Kelly, N.C. Price, J.G. Lindsay, Structure-function analysis of recombinant substrate protein 22 kDa (SP-22). A mitochondrial 2-CYS peroxiredoxin organized as a decameric toroid, J. Biol. Chem. 278 (2003) 32631–32637.
[17] A. Hall, K. Nelson, L.B. Poole, P.A. Karplus, Structure-based insights into the catalytic power and conformational dexterity of peroxiredoxins, Antioxid. Redox Signal. 15 (2011) 795–815.
[18] A. Hall, D. Parsonage, L.B. Poole, P.A. Karplus, Structural evidence that peroxiredoxin catalytic power is based on transition-state stabilization, J. Mol. Biol. 402 (2010) 194–209.
[19] H.H. Jang, S.Y. Kim, S.K. Park, H.S. Jeon, Y.M. Lee, J.H. Jung, S.Y. Lee, H.B. Chae, Y. J. Jung, K.O. Lee, et al., Phosphorylation and concomitant structural changes in human 2-Cys peroxiredoxin isotype I differentially regulate its peroxidase and molecular chaperone functions, FEBS Lett. 580 (2006) 351–355.
[20] H.H. Jang, K.O. Lee, Y.H. Chi, B.G. Jung, S.K. Park, J.H. Park, J.R. Lee, S.S. Lee, J. C. Moon, J.W. Yun, et al., Two enzymes in one; two yeast peroxiredoxins display oxidative stress-dependent switching from a peroxidase to a molecular chaperone function, Cell 117 (2004) 625–635.
[21] M. Jara, A.P. Vivancos, E. Hidalgo, C-terminal truncation of the peroxiredoxin Tpx1 decreases its sensitivity for hydrogen peroxide without compromising its role in signal transduction, Genes Cells: Devoted Mol. Cell. Mech. 13 (2008) 171–179.
[22] P.A. Karplus, A primer on peroxiredoxin biochemistry, Free Radic. Biol. Med. 80 (2015) 183–190.
[23] J. Konig, H. Galliardt, P. Jutte, S. Schaper, L. Dittmann, K.J. Dietz, The conformational bases for the two functionalities of 2-cysteine peroxiredoxins as peroxidase and chaperone, J. Exp. Bot. 64 (2013) 3483–3497.
[24] J. Konig, K. Lotte, R. Plessow, A. Brockhinke, M. Baier, K.J. Dietz, Reaction mechanism of plant 2-Cys peroxiredoxin. Role of the C terminus and the quaternary structure, J. Biol. Chem. 278 (2003) 24409–24420.
[25] K.H. Koo, S. Lee, S.Y. Jeong, E.T. Kim, H.J. Kim, K. Kim, K. Song, H.Z. Chae, Regulation of thioredoxin peroxidase activity by C-terminal truncation, Arch. Biochem. Biophys. 397 (2002) 312–318.
[26] J.C. Lim, H.I. Choi, Y.S. Park, H.W. Nam, H.A. Woo, K.S. Kwon, Y.S. Kim, S.G. Rhee, K. Kim, H.Z. Chae, Irreversible oxidation of the active-site cysteine of peroxiredoxin to cysteine sulfonic acid for enhanced molecular chaperone activity, J. Biol. Chem. 283 (2008) 28873–28880.
[27] F.M. Low, M.B. Hampton, A.V. Peskin, C.C. Winterbourn, Peroxiredoxin 2 functions as a noncatalytic scavenger of low-level hydrogen peroxide in the erythrocyte, Blood 109 (2007) 2611–2617.
[28] M. Molin, J. Yang, S. Hanzen, M.B. Toledano, J. Labarre, T. Nystrom, Life span extension and H(2)O(2) resistance elicited by caloric restriction require the peroxiredoxin Tsa1 in *Saccharomyces cerevisiae*, Mol. Cell 43 (2011) 823–833.
[29] J.C. Moon, Y.S. Hah, W.Y. Kim, B.G. Jung, H.H. Jang, J.R. Lee, S.Y. Kim, Y.M. Lee, M. G. Jeon, C.W. Kim, et al., Oxidative stress-dependent structural and functional switching of a human 2-Cys peroxiredoxin isotype II that enhances HeLa cell resistance to H_2O_2-induced cell death, J. Biol. Chem. 280 (2005) 28775–28784.
[30] J.C. Moon, G.M. Kim, E.K. Kim, H.N. Lee, B. Ha, S.Y. Lee, H.H. Jang, Reversal of 2-Cys peroxiredoxin oligomerization by sulfiredoxin, Biochem. Biophys. Res. Commun. 432 (2013) 291–295.
[31] M.A. Morais, P.O. Giuseppe, T.A. Souza, T.G. Alegria, M.A. Oliveira, L.E. Netto, M. T. Murakami, How pH modulates the dimer-decamer interconversion of 2-Cys peroxiredoxins from the Prx1 subfamily, J. Biol. Chem. 290 (2015) 8582–8590.
[32] K.J. Nelson, S.T. Knutson, L. Soito, C. Klomsiri, L.B. Poole, J.S. Fetrow, Analysis of the peroxiredoxin family: using active-site structure and sequence information for global classification and residue analysis, Proteins 79 (2011) 947–964.
[33] K.J. Nelson, D. Parsonage, A. Hall, P.A. Karplus, L.B. Poole, Cysteine pK(a) values for the bacterial peroxiredoxin AhpC, Biochemistry 47 (2008) 12860–12868.
[34] Y. Pan, J.H. Jin, Y. Yu, J. Wang, Significant enhancement of hPrx1 chaperone activity through lysine acetylation, Chembiochem: Eur. J. Chem. Biol. 15 (2014) 1773–1776.
[35] J.W. Park, G. Piszczek, S.G. Rhee, P.B. Chock, Glutathionylation of peroxiredoxin I induces decamer to dimers dissociation with concomitant loss of chaperone activity, Biochemistry 50 (2011) 3204–3210.
[36] D. Parsonage, D.S. Youngblood, G.N. Sarma, Z.A. Wood, P.A. Karplus, L.B. Poole, Analysis of the link between enzymatic activity and oligomeric state in AhpC, a bacterial peroxiredoxin, Biochemistry 44 (2005) 10583–10592.
[37] A.V. Peskin, F.M. Low, L.N. Paton, G.J. Maghzal, M.B. Hampton, C. C. Winterbourn, The high reactivity of peroxiredoxin 2 with H(2)O(2) is not reflected in its reaction with other oxidants and thiol reagents, J. Biol. Chem. 282 (2007) 11885–11892.
[38] T.J. Phalen, K. Weirather, P.B. Deming, V. Anathy, A.K. Howe, A. van der Vliet, T. J. Jonsson, L.B. Poole, N.H. Heintz, Oxidation state governs structural transitions in peroxiredoxin II that correlate with cell cycle arrest and recovery, J. Cell Biol. 175 (2006) 779–789.
[39] M. Radjainia, H. Venugopal, A. Desfosses, A.J. Phillips, N.A. Yewdall, M. B. Hampton, J.A. Gerrard, A.K. Mitra, Cryo-electron microscopy structure of human peroxiredoxin-3 filament reveals the assembly of a putative chaperone, Structure 23 (2015) 912–920.
[40] F. Saccoccia, P. Di Micco, G. Boumis, M. Brunori, I. Koutris, A.E. Miele, V. Morea, P. Sriratana, D.L. Williams, A. Bellelli, et al., Moonlighting by different stressors: crystal structure of the chaperone species of a 2-Cys peroxiredoxin, Structure 20 (2012) 429–439.
[41] G.N. Sarma, C. Nickel, S. Rahlfs, M. Fischer, K. Becker, P.A. Karplus, Crystal structure of a novel *Plasmodium falciparum* 1-Cys peroxiredoxin, J. Mol. Biol. 346 (2005) 1021–1034.
[42] R.S. Sikorski, P. Hieter, A system of shuttle vectors and yeast host strains designed for efficient manipulation of DNA in *Saccharomyces cerevisiae*, Genetics 122 (1989) 19–27.
[43] L. Soito, C. Williamson, S.T. Knutson, J.S. Fetrow, L.B. Poole, K.J. Nelson, PREX: PeroxiRedoxin classification indEX, a database of subfamily assignments across the diverse peroxiredoxin family, Nucleic Acids Res. 39 (2011) D332–D337.
[44] F. Teixeira, H. Castro, T. Cruz, E. Tse, P. Koldewey, D.R. Southworth, A.M. Tomas, U. Jakob, Mitochondrial peroxiredoxin functions as crucial chaperone reservoir in *Leishmania infantum*, Proc. Natl. Acad. Sci. USA 112 (2015) E616–E624.
[45] H.A. Woo, H.Z. Chae, S.C. Hwang, K.S. Yang, S.W. Kang, K. Kim, S.G. Rhee, Reversing the inactivation of peroxiredoxins caused by cysteine sulfinic acid formation, Science 300 (2003) 653–656.
[46] Z.A. Wood, L.B. Poole, R.R. Hantgan, P.A. Karplus, Dimers to doughnuts: redox-sensitive oligomerization of 2-cysteine peroxiredoxins, Biochemistry 41 (2002) 5493–5504.
[47] Z.A. Wood, L.B. Poole, P.A. Karplus, Peroxiredoxin evolution and the regulation of hydrogen peroxide signaling, Science 300 (2003) 650–653.
[48] Z.A. Wood, E. Schroder, J. Robin Harris, L.B. Poole, Structure, mechanism and regulation of peroxiredoxins, Trends Biochem. Sci. 28 (2003) 32–40.
[49] K.S. Yang, S.W. Kang, H.A. Woo, S.C. Hwang, H.Z. Chae, K. Kim, S.G. Rhee, Inactivation of human peroxiredoxin I during catalysis as the result of the oxidation of the catalytic site cysteine to cysteine-sulfinic acid, J. Biol. Chem. 277 (2002) 38029–38036.